

Self-energy effects on the surface-state energies of H-Si(111)1×1

X. Blase

Department of Physics, University of California at Berkeley and Materials Sciences Division, Lawrence Berkeley Laboratory, Berkeley, California 94720

Xuejun Zhu

*Department of Physics, University of California at Berkeley and Materials Science Division, Lawrence Berkeley Laboratory, Berkeley, California 94720
and AT&T Bell Laboratories, Murray Hill New Jersey 07974*

Steven G. Louie

Department of Physics, University of California at Berkeley and Materials Sciences Division, Lawrence Berkeley Laboratory, Berkeley, California 94720

(Received 25 August 1993)

We have calculated the quasiparticle energy of the occupied surface states of the H-Si(111)1×1 surface. The electron self-energy operator is expanded to first order in the screened Coulomb interaction in the *GW* approximation. The results explain the data from recent high-resolution angle-resolved photoemission spectroscopy. Comparison of the quasiparticle surface-state energies with those from local-density-functional eigenvalues shows that the self-energy corrections are very large, typically two to three times larger than the corrections found in previous calculations on other semiconductor surface systems. We have also performed a frozen-phonon study of the stretching mode of the Si-H bond. As observed in several recent experiments and theoretical studies, a large anharmonicity is found.

I. INTRODUCTION

Recently, the development of a wet chemical treatment^{1,2} has allowed the preparation of very flat, highly stable, and nearly defect-free hydrogen-terminated Si(111) surfaces. The quality of these surfaces is characterized by the exceptionally small linewidth of electronic and vibrational states in photoemission³ and vibrational^{1,2,4} spectroscopy experiments. This has generated much renewed interest in this system since measurements can now unravel very fine structures in the spectroscopic data with very little inhomogeneity or impurity broadening.

The present work is motivated by a recent high-resolution angle-resolved photoemission spectroscopy (ARPES) experiment performed on such an "ideal" H-Si(111)1×1 surface.⁵ The spectra were obtained using the French-Swiss beam line (SU3) at SuperACO in LURE.⁶ The quality of the surface, combined with a state-of-the-art instrumental resolution (25 meV for valence states), yields surface states in the ARPES data with a typical linewidth of 300 meV, much smaller than those measured with samples from other preparation methods such as by adsorbing atomic hydrogen on freshly cleaved Si(111) surfaces⁷ or those of the ideally H-terminated Si(111)1×1 surfaces obtained by removal of an indium adalayer by atomic hydrogen.⁸

In this paper, we address mainly the issue of the surface states located in the Si valence bands. Surface states in the conduction bands have also been previously stud-

ied experimentally and theoretically⁹ but these states are weak resonances. Surface states in the valence bands of the H/Si(111) surface have been examined in several previous calculations.⁹⁻¹² Although the character of these states is qualitatively understood, discrepancies in their energy locations as large as 1 eV were found between theory and experiment. This is because the previous studies were either semiempirical¹⁰⁻¹² in nature or were based on the local-density approximation⁹ (LDA) which does not provide an accurate description of the quasiparticle energies measured in the photoemission process.

In order to make a direct comparison with the experimental data, we present here a first-principles calculation of the quasiparticle surface-state energies. The computation of the quasiparticle energies is achieved using a quasiparticle self-energy method,¹³ based on the *GW* approximation^{14,15} which has been shown to yield for semiconductors bulk,^{13,16,17} surface,¹⁸⁻²¹ interface,²² and superlattice²³ quasiparticle energies accurate to within 0.1 eV when compared to experiment. The method has also been successfully applied to complex materials such as solid C₆₀ recently.²⁴

The remainder of this paper is organized as follows: In Sec. II, we discuss the theoretical methods employed in this study. The *ab initio* pseudopotential method employing a plane-wave basis set in a supercell slab geometry was used to determine the surface structure and vibrational properties of the Si-H stretching mode. The bulk and surface-state energies were calculated using the first-principles quasiparticle approach. In Sec. III, the theoretical results are presented and compared with data

from spectroscopic measurements. Finally, a summary and conclusions are given in Sec. IV.

II. THEORETICAL METHODS

A. LDA *ab initio* pseudopotential total energy calculations

The LDA calculations were carried out using *ab initio* pseudopotentials. For Si, we use the Hamann-Schlüter-Chiang pseudopotential scheme.²⁵ For hydrogen, the pseudopotential is obtained using a modified Kerker scheme²⁶ based on the inversion of the exact hydrogenic Schrödinger equation. This scheme provides a very smooth pseudopotential for hydrogen with excellent transferability. The Ceperley-Alder exchange and correlation potential²⁷ was used. The potentials and eigenstates are expanded in a plane-wave basis. The calculations were carried out using a cutoff of $E_{\text{cut}} = 16$ Ry in the plane-wave expansion of the wave functions. This cutoff corresponds to an average of 2200 plane waves in the basis set for the surface calculation described below. We exploited an iterative diagonalization technique²⁸ to calculate the desired lowest eigenstates. A $4 \times 4 \times 1$ grid in the Monk-Pack scheme²⁹ was used to generate ten special k points in the irreducible part of the two-dimensional surface Brillouin zone (SBZ).

In each supercell, we have a 12-layer Si slab terminated by hydrogen saturating the dangling bond on each side. With this geometry, our slab retains inversion symmetry. The vacuum between adjacent slabs was chosen to be 12 a.u. This vacuum region is large enough as confirmed by the absence of dispersion for the slab band structure in the direction normal to the surface and by the flatness of the total potential in the middle of the vacuum region. We checked also the convergence in the thickness of the slab: The overlap through the slab for the surface states located on two hydrogen atoms on the opposite side induces a splitting of the surface-state energies which is at most 0.1 eV. The surface-state energies given below are taken to be simple algebraic average of the energy of the split levels.

For the specific study of the Si-H stretching mode, we increased the energy cutoff up to $E_{\text{cut}} = 20$ Ry: Going from 16 Ry to 20 Ry reduces the fundamental frequency by 8%.

B. First-principles quasiparticle approach to electron excitation energies

The computation of the quasiparticle energies is achieved using a self-energy approach.^{13,14} In this formalism, the Schrödinger-like equation solved to obtain the one-particle excitation energies E_{QP} is given by

$$\begin{aligned} & [\hat{T} + V_{\text{ext}}(\mathbf{r}) + V_H(\mathbf{r})]\Psi^{\text{QP}}(\mathbf{r}) \\ & + \int d\mathbf{r}' \Sigma(\mathbf{r}, \mathbf{r}'; E^{\text{QP}})\Psi^{\text{QP}}(\mathbf{r}') = E^{\text{QP}}\Psi^{\text{QP}}(\mathbf{r}), \end{aligned} \quad (1)$$

where \hat{T} is the kinetic energy operator, V_{ext} the external potential, and V_H a mean-field electron-electron interaction potential (the Hartree potential in this case.) The self-energy operator Σ includes the effects of exchange and correlation: It is nonlocal, energy dependent, and non-Hermitian in general.

In the *GW* approximation¹⁵ used in this calculation, Σ is taken to be the first-order term in an expansion in successive powers of the screened interaction W :

$$\begin{aligned} \Sigma(\mathbf{r}, \mathbf{r}'; E^{\text{QP}}) &= i \int \frac{dE'}{2\pi} e^{-i\delta E'} G(\mathbf{r}, \mathbf{r}'; E - E') \\ &\quad \times W(\mathbf{r}, \mathbf{r}'; E'), \end{aligned} \quad (2)$$

where G is the dressed one-particle Green's function. Our approach¹³ is to make the best possible approximation for G and W . As shown in previous *GW* calculations in semiconductors, the LDA wave functions accurately describe the quasiparticle wave functions in semiconductors so that we may write

$$G(E) = \sum_{n\mathbf{k}} \frac{|n\mathbf{k}\rangle\langle n\mathbf{k}|}{E - E_{n\mathbf{k}} - i\eta}, \quad (3)$$

with $|n\mathbf{k}\rangle$ the LDA eigenfunctions and $E_{n\mathbf{k}}$ the self-consistent quasiparticle energies (η is a negative infinitesimal for energies above the Fermi energy and a positive infinitesimal below).

The screened Coulomb interaction $W = V\epsilon^{-1}$ is calculated in Fourier space using the Hybertsen-Louie scheme.^{13,30} V is the bare Coulomb potential and ϵ^{-1} the inverse dynamical dielectric matrix. In calculating ϵ^{-1} , the static polarizability P is evaluated in the Adler-Wiser formulation^{31,32} within the random-phase approximation (RPA). Local field effects are taken into account so that the polarizability matrix is nondiagonal in reciprocal space. This is the most time-consuming part of our scheme. After inversion of the static dielectric matrix $\epsilon(\mathbf{q}, \omega = 0)$, we extend ϵ^{-1} to finite frequencies using a generalized plasmon pole model³⁰ which yields a different pole at $\tilde{\omega}_{\mathbf{G}, \mathbf{G}'}(\mathbf{q})$ for each element $\epsilon_{\mathbf{G}, \mathbf{G}'}^{-1}(\mathbf{q}; \omega)$ of the inverse dielectric matrix. The strength and position of each pole are uniquely determined by imposing that $\epsilon_{\mathbf{G}, \mathbf{G}'}^{-1}(\mathbf{q}; \omega)$ satisfy both the Kramers-Kronig relations and a generalized f -sum rule.¹³

The quasiparticle excitation energies are then calculated using first-order perturbation theory:

$$E_{n\mathbf{k}}^{\text{QP}} = E_{n\mathbf{k}}^{\text{LDA}} + \langle n\mathbf{k} | \Sigma(E_{n\mathbf{k}}^{\text{QP}}) - V^{\text{LDA}} | n\mathbf{k} \rangle. \quad (4)$$

The validity of Eq. (4) is based on the fact that the LDA and quasiparticle wave functions are, in general, in excellent agreement.¹³ Thus, one needs only to calculate the diagonal elements of the difference Hamiltonian $\Sigma(E_{n\mathbf{k}}^{\text{QP}}) - V^{\text{LDA}}$.

In the calculation, the static polarizability $P(\mathbf{q}, \omega = 0)$ was evaluated using ten special \mathbf{q} points in the irreducible part of the SBZ with a special treatment for the $\bar{\Gamma}$ point (Ref. 30, Appendix A). The $P_{\mathbf{G}, \mathbf{G}'}$ matrix elements were calculated for $|\mathbf{q} + \mathbf{G}| < 3.4$ a.u. which yields dielectric matrices of average size of 200×200 for each special \mathbf{q}

point. This is sufficient to describe the local field effects in the dielectric screening in the present case. We also included transitions up to 350 conduction bands for each \mathbf{k} point.

The calculation of the self-energy matrix elements¹³ requires a smaller cutoff: We used $|\mathbf{q} + \mathbf{G}| < 2.8$ a.u. to converge the bare exchange energies and $|\mathbf{q} + \mathbf{G}| < 2.1$ a.u. for the dynamical part of Σ . Over 350 bands in the summation over conduction states were used for the Coulomb-hole term. With these cutoffs, the self-energies are found to converge to within 0.1 eV.

III. RESULTS AND ANALYSIS

A. Structure and H-Si stretching mode

By total energy minimization within LDA, we find that the Si-H bond length for the unreconstructed surface is 2.87 a.u., in good agreement with previous calculations [2.80 a.u. (Ref. 9) and 2.90 a.u. (Ref. 33)]. For the silicon substrate, we start with the experimental bulk silicon lattice constant. The first layer is found to be slightly relaxed inward by 0.075 a.u. while relaxation of deeper layers is negligible. The inward relaxation of the first layer is 0.03 a.u. larger than the value calculated in Ref. 33: The difference in the number of layers, width of the vacuum space, and k -point sampling may account for this discrepancy which has only a very small effect on the total energy. The position of the surface states and the parameters of the Si-H stretching are insensitive to such a small variation in the first layer relaxation.

The stretching mode of the Si-H bond was investigated using the method of Ref. 34. We find that the hydrogen moves in a potential well (see Fig. 1) which can be well

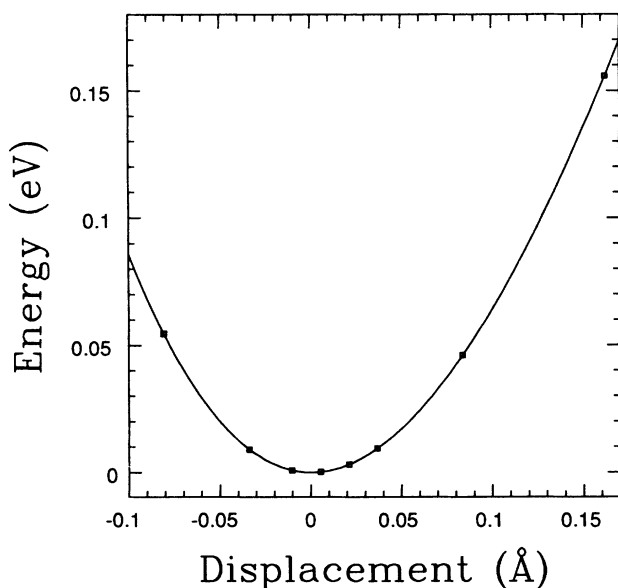


FIG. 1. Calculated potential well of H-Si bond as a function of the displacement from equilibrium bond length. The open squares are the calculated points and the solid line is a fourth-order polynomial least-squares fit.

described using the following fourth-order polynomial expression:

$$V(z) = V_0 + 0.543z^2 - 0.781z^3 + 0.771z^4, \quad (5)$$

where the energies are in Ry and z is the deviation from equilibrium of the Si-H bond length in angstroms. With this potential, we find a harmonic frequency of $\hbar\Omega_0 = 251.2$ meV (2025.0 cm^{-1}) and the difference between the overtone frequency and twice $\hbar\Omega_0$ to be $-2\Gamma = 4.1$ meV (33.4 cm^{-1}) in excellent agreement with the theoretical value in Ref. 33 in the case when no coupling with the wagging modes is considered. As described in Ref. 33, these values can be successfully used as parameters to describe phonon-phonon interactions through a negative- U Hubbard-type Hamiltonian which yields an excellent value for the binding energy of the two-phonon bound state recently observed³⁵ in this system.

B. Surface-state energies

The results of the LDA and quasiparticle surface-state band structure calculations are presented in Fig. 2. In the background is the continuum of Si bulk quasiparticle states projected along the (111) direction onto the SBZ. For each \bar{k} parallel to the surface (along $\bar{\Gamma}-\bar{K}-\bar{M}-\bar{\Gamma}$), we projected the energy levels of the quasiparticle bulk states of 100 regularly spaced \mathbf{k} points of the bulk fcc Brillouin zone. This presentation of the projected quasiparticle band structure, in contrast to a uniform shading of the bulk continuum, allows the detection of lines of high density of bulk states in the continuum. They are in excellent agreement with the ARPES data⁵ and are valuable in identifying bulk peaks as compared to surface

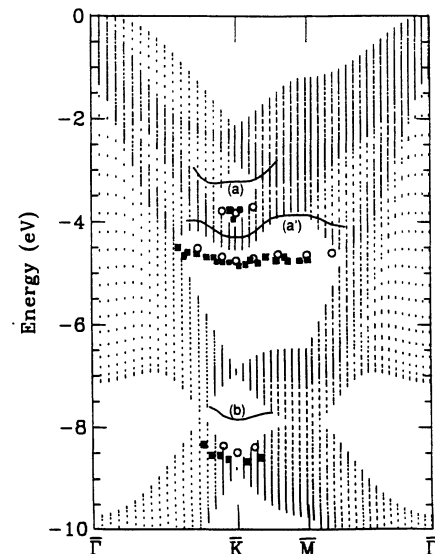


FIG. 2. Surface-state bands calculated within LDA (solid lines) and GW (open circles). The solid squares represent the experimental data (Ref. 5). In the background is the projected Si bulk GW band structure. The zero of the energy scale is at the top of the valence band.

related peaks in spectroscopic data. These bulk states are calculated in the framework of our first-principles quasiparticle approach using the usual diamond-structure unit cell of bulk silicon. The calculated pockets in the projected bulk band structure are in excellent agreement with experiment.

1. LDA results

In Fig. 2, the LDA surface-state eigenvalues are given by the solid lines while the experimental values⁵ are given by the solid squares. Well-defined surface states exist in each local gap (or pocket) of the projected bulk band structure near \bar{K} and \bar{M} . These states have wave functions which are highly localized at the surface [Figs. 3(a,c,d)]. The states (*a*) at \bar{K} [Fig. 3(a)] and (*a'*) at \bar{M} [Fig. 3(d)] are the results of the hybridization of the Si $3p_z$ orbital with the H $1s$ orbital, while interactions of the Si $3s$ and the H $1s$ orbitals are responsible for the low-lying surface states (*b*) at -7.85 eV at \bar{K} . The enhancement of the \mathbf{k} -resolved local density of states (LDOS) on the first H layer at the calculated surface-state energies as compared to the bulk density of states (DOS) at \bar{K} and \bar{M} [Figs. 4(b,c)] further illustrates the localized character of these states. The state (*a'*) at \bar{K} is found in the LDA calculations to be within the bulk continuum but of a different symmetry than the surrounding bulk states. The corresponding wave function [see Fig. 3(b)] is very delocalized as compared to the state (*a'*) at \bar{M} . However, an analysis of the symmetry of this state clearly shows that this state is hydrogen induced and is the continuation of the *bona fide* surface band (*a'*) along \bar{K} to \bar{M} . An angular decomposition of the wave function around the hydrogen atom and the first layer silicon atom showed distinctly a different character for this state from that of surrounding bulk states: The states (*a'*) at \bar{M} and \bar{K} have the same character at the surface.

To examine whether the larger delocalization of the surface state (*a'*) at \bar{K} is the result of being incorrectly positioned within LDA, we performed a Slater-Koster³⁶ tight-binding (TB) calculation on our 12-Si-layer slab using Pandey's nearest and second nearest neighbor parameters.¹¹ [The TB results do not yield a surface resonance for the surface state (*a'*) at \bar{K} .] We compared first our tight-binding surface-state energies with Pandey's results for a 36-Si-layer slab. The results are quoted in Table I. The energies of the surface states as given by the two TB calculations differ by less than 0.11 eV (which also confirms that our slab is thick enough). Consistent with Pandey's findings, our tight-binding calculation locates the state (*a'*) at \bar{K} well within the small pocket of the projected bulk continuum. Moreover, in agreement with our LDA calculations, the wave function at \bar{K} is much less localized than that at \bar{M} : Only 35% of the wave function is localized on the two outermost layers at \bar{K} as compared to 69% at \bar{M} . This shows that, because of symmetry, the state (*a'*) hardly resonates with the nearby bulk states at \bar{K} and that the corresponding

TABLE I. Energies of surface states at \bar{K} and \bar{M} (in eV with zero at the top of the valence band).

k point	Tight binding	Present calculations			Expt.
	(Ref. 11)	TB	LDA	GW	(Ref. 5)
\bar{K}	-3.88	-3.82	-3.22	-3.82	-3.80
	-5.02	-4.94	-4.29	-4.76	-4.78
	-8.83	-8.94	-7.85	-8.47	-8.64
\bar{M}	-4.94	-4.86	-3.87	-4.63	-4.76

delocalization of the wave function is rather insensitive to its position in energy as compared to the bulk continuum edge. This will be of some importance in our self-energy calculation which assumes that the LDA and quasiparticle wave functions are in good agreement.

The LDOS at $\bar{\Gamma}$ is given in Fig. 4(a): The features in the LDOS for the center of the slab from -7 eV to -2 eV illustrate the finite size effects related to the slab geometry, but the enhancement of some of these structures in the H layer LDOS indicates that surface resonances exist in this energy range as reported in previous calculations^{9,11,12}

The LDA energies of the surface states at \bar{K} and \bar{M} are also reported in Table I. As compared to experiment, LDA underbinds the occupied surface states. This is consistent with previous calculations³⁸ for other surfaces, but the effect is significantly larger in the present case. This is related to the very localized $1s$ hydrogen orbital forming the surface states in the present system: Figure 3 shows that the wave functions of the bonding surface states are not centered in the middle of the H-Si bond but fall into the deep well created by the hydrogen nucleus. The discrepancy in the energy position between LDA and experiment for the state (*a'*) at \bar{M} and the state (*b*) at \bar{K} is larger by a factor 2–3 as compared to that for surface states at the As-Si(111) surface.¹⁹ This difference between the two systems can be partially understood by examining the atomic calculations. Figure 5 shows the error in the LDA eigenvalue energy for the highest occupied state as compared to the experimental ionization energy. It is well known that the discrepancy is very large for all atoms.³⁷ This error resulting from using LDA exchange-correlation potential as an approximation to the self-energy operator is therefore large. In the case of surface-state energies, we are interested in their relative position to bulk states. Thus the energy differences between substrate and adsorbate levels are important. The cancellation of error is much more favorable in the As-Si system than the H-Si system. These differences are quoted in Table II. One can see that the discrepancy is even worse for the energy difference H($1s$)-Si($3s$): This is relevant for the state (*c*) at \bar{K} .

In addition to not yielding the correct position of surface states relative to bulk states, LDA in the present case does not give the correct dispersion for the surface states. For example, for the surface band (*a'*) between \bar{M} and \bar{K} , while the experimental data do not show any dispersion, the LDA calculation gives a dispersion of 0.42 eV.

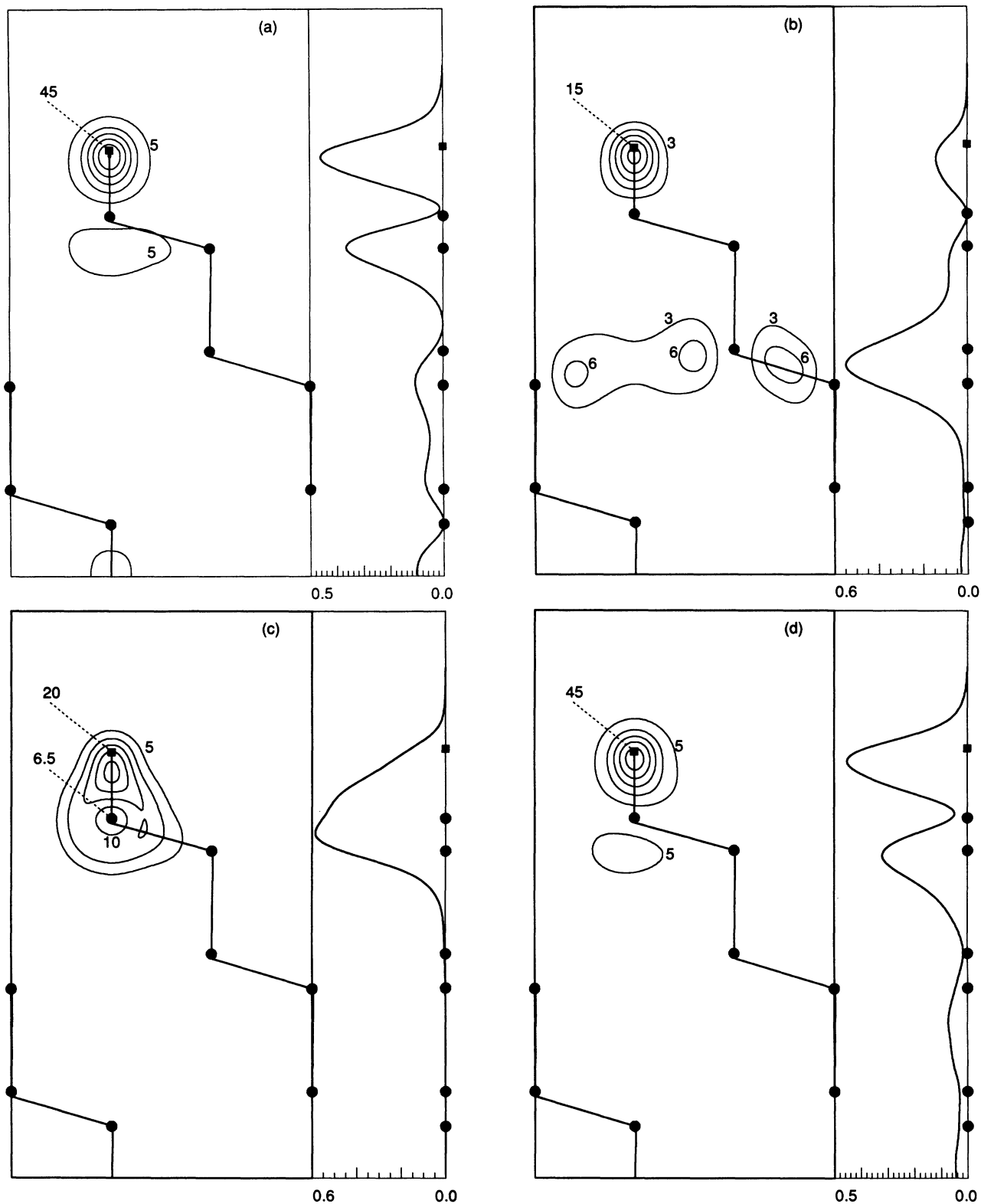


FIG. 3. Contour plot in the [110] plane of selected surface-state wave functions and corresponding xy -averaged charge density plotted along the surface normal direction z . The values which label the contours correspond to $(2\pi)^3|\psi|^2$ where ψ is the corresponding wave function normalized such that $\int_{\Omega_c} dV |\psi|^2 = 1$, with Ω_c the unit cell volume. The xy -average charge density is normalized to unity within one unit cell. (a), (b), (c), and (d) correspond, respectively, to the LDA calculated states at -3.22 eV, -4.29 eV, -7.85 eV at \bar{K} and the state at -3.87 eV at \bar{M} . The wave functions are plotted from the middle of the slab to the middle of the vacuum. The dots represent the silicon atoms contained in the [110] plane and the squares represent the hydrogen atoms. The dashed lines point to the charge density on the hydrogen or silicon atom.

TABLE II. Energy difference between selected LDA atomic levels for Si, As, and H as compared to experiment. The energies are given in eV.

	H(1s)-Si(3p)	As(4p)-Si(3p)	H(1s)-Si(3s)	As(4p)-Si(3s)
LDA	-2.17	-1.2	4.48	5.46
Expt.	-5.45 ^a	-1.6 ^a	-0.14 ^a	3.65 ^b

^aReference 39.

^bReference 40.

2. Quasiparticle results

Because spectroscopic measurements can be understood in terms of excitations between quasiparticle states of the interacting electron system, our quasiparticle self-energy approach yields results in much better agreement with photoemission data than LDA. In the present case, very large self-energy corrections to the position of the LDA surface states are found: The self-energy corrections for the state (*a'*) at \bar{M} and the state (*b*) at \bar{K} are 2–3 times larger than those for the surface states at the As-Si(111) surface.¹⁹ This can be understood from the important nonlocal and dynamical effects induced by the high degree of localization of the surface states in the H-Si system. For selected *k* points of the surface Brillouin zone, our calculated quasiparticle energy levels are given in Fig. 2 by the open circles. The specific energy levels

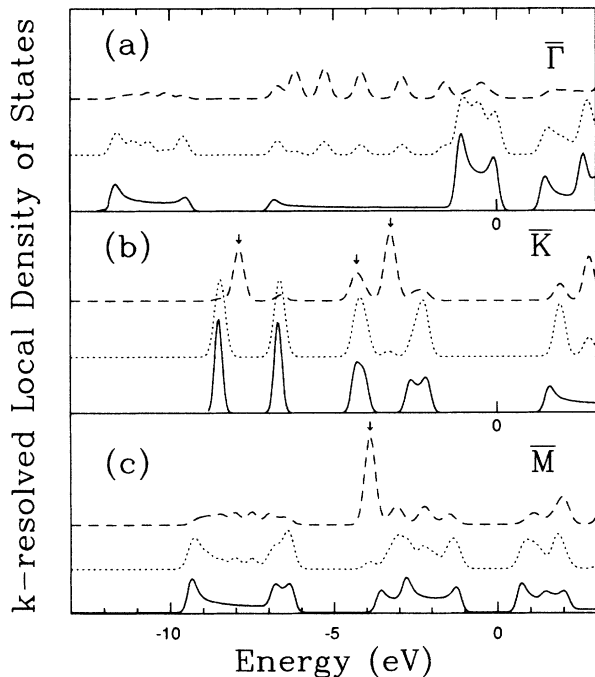


FIG. 4. *k*-resolved LDOS for selected \bar{k} points as calculated in the LDA. The solid line correspond to the bulk DOS. The upper long-dashed line corresponds to the H-layer LDOS and the middle short-dashed line to the “center of the slab” LDOS (innermost four Si layers included). The arrows indicate the position of the surface states as given by the LDA eigenvalues (see Table I).

for the surface states at \bar{K} and \bar{M} are quoted in Table I. The agreement between our quasiparticle theory and the recent ARPES experiment is excellent: The discrepancy is at most 0.17 eV for the higher binding energy surface state at \bar{K} . This is much smaller than the 0.79 eV discrepancy for this state as calculated within LDA.

As a consequence of the improvement in the overall position of the surface states, the self-energy approach yields also an impressive improvement in the dispersion of all the surface states. This again may be understood from the sensitivity of the self-energy operator to the localization of the surface states. We compare in Fig. 6 the exchange-correlation energies for different states of the band (*a'*) between \bar{K} and \bar{M} as given by different approximations. The bare Fock exchange, the LDA and the *GW* exchange-correlation operators have very different *k*-dependent behavior. Recall that the surface state (*a'*) is more localized at \bar{M} than at \bar{K} . The LDA exchange-correlation operator is much less sensitive to localization than the self-energy operator Σ and thus underestimates by 0.3 eV the dispersion of the exchange-correlation energy for the band (*a'*) between \bar{K} and \bar{M} . As expected, the bare exchange operator, which neglects screening effects, overestimates the dispersion. In contrast to both the LDA and bare exchange approximation, the self-energy approach yields a dispersion which is in almost perfect agreement with ARPES data.

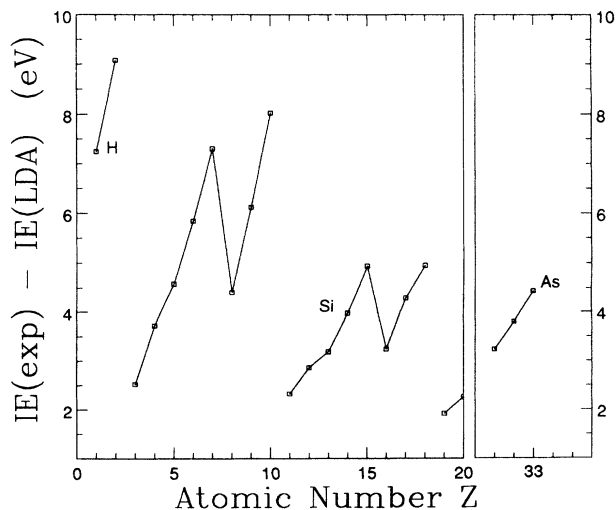


FIG. 5. Difference between the LDA highest occupied state eigenvalue and the experimental ionization energy (in eV) for selected elements of the Periodic Table.

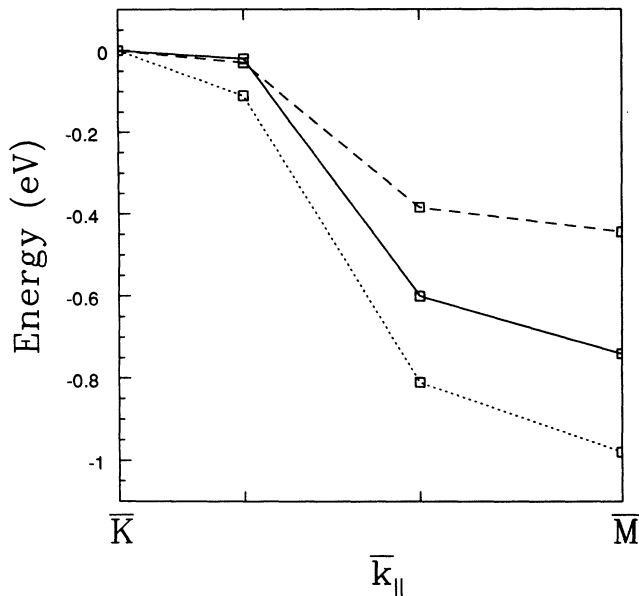


FIG. 6. Energy dispersion for different approximations to the exchange-correlation operators for the surface-state band (a') at selected points between \bar{K} and \bar{M} . The zero of energy scale is taken at \bar{K} . The solid line corresponds to the GW self-energy Σ operator, the dashed line to the LDA operator, and the dotted line to the bare exchange operator. The open squares are the points where the energies have been calculated (in eV).

The self-energy operator is also more sensitive to wavefunction character as a consequence of its nonlocality. The state (a') at \bar{K} , which differs from surrounding bulk states by its strong hydrogenic character at the surface, is successfully extracted from the bulk continuum by the self-energy approach. It is important to note that even in the tight-binding calculation which locates the surface state (a') at \bar{K} well within a pocket, the wave function at \bar{K} is still much less localized than at \bar{M} . This shows that the wave function (a') at \bar{K} does not change when extracted from the bulk continuum and the use of the LDA wave function to describe the quasiparticle wave function for this state is valid.

The small discrepancy between theory and experiment for the surface states at higher binding energy near \bar{K} could be due to several effects. First, because the static part of the dielectric function is calculated exactly within the RPA, we expect the generalized plasmon pole model

used to extend the dielectric function to finite frequency to be more accurate in the low-energy range. Therefore, the self-energy of the smaller binding energy states are the most accurate within our scheme. Second, we neglect the influence of finite lifetime effects on the position of the quasiparticle energies. Since states closer to the gap edges have a larger lifetime, we expect these effects to be more important for states at higher binding energy. We emphasize that these discrepancies are small: The discrepancy is within the combined uncertainties of GW theory and experiment.

IV. CONCLUSION

We calculated within the GW approximation the quasiparticle energies for occupied surface states of the H-Si(111)1 \times 1 surface. This approach yields quasiparticle energies in excellent agreement with a recent high-resolution angle-resolved photoemission spectroscopy performed on the "ideally" prepared surface. The ability of our first-principles quasiparticle approach to describe the dynamical and nonlocal effects in this highly anisotropic system, exhibiting very localized states on the Si-H bond, has been exemplified. Our LDA calculations also confirm that LDA combined with a slab model can accurately describes the ground-state properties of such surfaces and that the LDA wave functions are an excellent starting point for quasiparticle calculations in the Hybertsen-Louie formulation within the GW approximation.

ACKNOWLEDGMENTS

We thank Dr. Yves Petroff for making his photoemission data on H-Si(111)1 \times 1 available to us and for many useful discussions. We acknowledge also Christian Elsässer who made available to us his modified Kerker scheme to generate the H pseudopotential. One of us (X.B.) would like to thank Eric Shirley for useful discussions and encouragements. This work was supported by National Science Foundation Grant No. DMR-9120269 and by the Director, Office of Energy Research, Office of Basic Energy Sciences, Materials Sciences Division of the U.S. Department of Energy under Contract No. DE-AC03-76SF00098. Supercomputer time was provided by the NSF Pittsburgh Supercomputer Center.

¹ G. S. Higashi *et al.*, Appl. Phys. Lett. **56**, 656 (1990); **58**, 1656 (1991).

² P. Guyot-Sionnest, P. Dumas, Y. J. Chabal, and G. S. Higashi, Phys. Rev. Lett. **64**, 2156 (1990); P. Dumas, Y. J. Chabal, and G. S. Higashi, *ibid.* **65**, 1124 (1990); P. Guyot-Sionnest, *ibid.* **66**, 1489 (1991).

³ S. Bouzidi *et al.*, Phys. Rev. B **45**, 1187 (1992).

⁴ P. Jakob *et al.*, Appl. Phys. Lett. **59**, 2968 (1991); Chem. Phys. Lett. **187**, 325 (1991).

⁵ K. Hricovini *et al.*, Phys. Rev. Lett. **70**, 1992 (1993).

⁶ Laboratoire pour l'Utilisation du Rayonnement Electromagnetique, Centre Universitaire Paris-Sud-Bat.209D-F91405 Orsay Cedex (France).

⁷ C. J. Karlsson *et al.*, Phys. Rev. B **41**, 1521 (1990).

- ⁸ E. Landemark, C. J. Karlsson, and R. I. G. Uhrberg, *Phys. Rev. B* **44**, 1950 (1991).
- ⁹ M. B. Nardelli *et al.*, *Surf. Sci.* **269/270**, 879 (1992).
- ¹⁰ J. A. Appelbaum and D. R. Hamann, *Phys. Rev. Lett.* **34**, 806 (1975).
- ¹¹ K. C. Pandey, T. Sakurai, and H. D. Hagstrum, *Phys. Rev. Lett.* **35**, 1728 (1975).
- ¹² K. M. Ho, M. L. Cohen, and M. Schlüter, *Phys. Rev. B* **15**, 3888 (1977).
- ¹³ M. S. Hybertsen and S. G. Louie, *Phys. Rev. Lett.* **55**, 1418 (1985); *Phys. Rev. B* **34**, 5390 (1986).
- ¹⁴ L. Hedin and S. Lunqvist, in *Solid State Physics: Advances in Research and Applications*, edited by F. Seitz, D. Turnbull, and H. Ehrenreich (Academic, New York, 1969), Vol. 23.
- ¹⁵ L. Hedin, *Phys. Rev.* **139**, A796 (1965).
- ¹⁶ R. W. Godby, M. Schlüter, and L. J. Sham, *Phys. Rev. Lett.* **56**, 2415 (1986); *Phys. Rev. B* **36**, 6497 (1987); **37**, 10 159 (1988).
- ¹⁷ X. Zhu and S. G. Louie, *Phys. Rev. B* **43**, 14 142 (1991).
- ¹⁸ M. S. Hybertsen and S. G. Louie, *Phys. Rev. B* **38**, 4033 (1988).
- ¹⁹ R. S. Becker, B. S. Swartzentruber, J. S. Vickers, M. S. Hybertsen, and S. G. Louie, *Phys. Rev. Lett.* **60**, 116 (1988).
- ²⁰ J. E. Northrup, M. S. Hybertsen, and S. G. Louie, *Phys. Rev. Lett.* **66**, 500 (1991).
- ²¹ X. Zhu and S. G. Louie, *Phys. Rev. B* **43**, 12 146 (1991).
- ²² S. B. Zhang, D. Tománek, S. G. Louie, M. L. Cohen, and M. S. Hybertsen, *Solid State Commun.* **66**, 585 (1988).
- ²³ M. S. Hybertsen and M. Schlüter, *Phys. Rev. B* **36**, 9683 (1987); S. B. Zhang, M. S. Hybertsen, M. L. Cohen, S. G. Louie, and D. Tománek, *Phys. Rev. Lett.* **63**, 1495 (1989).
- ²⁴ E. Shirley and S. G. Louie, *Phys. Rev. Lett.* **71**, 133 (1993).
- ²⁵ D. R. Hamann, M. Schlüter, and C. Chiang, *Phys. Rev. Lett.* **43**, 1494 (1979).
- ²⁶ G. P. Kerker, *J. Phys. C* **13**, L189 (1980); K. M. Ho, C. Elsässer, C. T. Chan, and M. Fähnle, *J. Phys. Condens. Matter* **4**, 5189 (1992).
- ²⁷ D. M. Ceperley and B. J. Alder, *Phys. Rev. Lett.* **45**, 566 (1980).
- ²⁸ R. Natarajan and D. Vanderbilt, *J. Comput. Phys.* **81**, 218 (1989).
- ²⁹ H. J. Monkhorst and J. D. Pack, *Phys. Rev. B* **13**, 5188 (1976).
- ³⁰ M. S. Hybertsen and S. G. Louie, *Phys. Rev. B* **35**, 5585 (1987).
- ³¹ S. L. Adler, *Phys. Rev.* **126**, 413 (1962).
- ³² N. Wisser, *Phys. Rev.* **129**, 62 (1963).
- ³³ X. P. Li and D. Vanderbilt, *Phys. Rev. Lett.* **69**, 2543 (1992).
- ³⁴ X. Zhu and S. G. Louie, *Phys. Rev. B* **45**, 3940 (1992).
- ³⁵ P. Guyot-Sionnest, *Phys. Rev. Lett.* **67**, 2323 (1991).
- ³⁶ J. C. Slater and G. F. Koster, *Phys. Rev.* **94**, 1498 (1954).
- ³⁷ R. O. Jones and O. Gunnarsson, *Rev. Mod. Phys.* **61**, 689 (1989), and references therein.
- ³⁸ This is illustrated in S. G. Louie, in *Electronic Structure, Dynamic and Quantum Structural Properties of Condensed Matter*, edited by J. Devreese and P. van Camp (Plenum, New York, 1985), p. 335.
- ³⁹ C. Kittel, *Introduction to Solid State Physics*, 6th ed. (Wiley, New York, 1986), Table 5, p. 59.
- ⁴⁰ S. Bashkin and J. O. Stoner, *Atomic Energy Levels and Grotian Diagrams* (North-Holland, New York, 1975), Vol. 1. We estimate the experimental Si 3s eigenvalue by adding the experimental first ionization energy to the promotion energy $s^2p(^2P) \rightarrow sp^2(^4P)$. We neglect therefore relaxation effects which are for these levels not larger than some few tenths of eV.